



# Master sintering curve analysis of ZnO densified by Cold Sintering Process

Nicolas Albar, Thomas Hérissou de Beauvoir, Aurélien Bouyat, Geoffroy Chevallier, Alicia Weibel, Claude Estournès

## ► To cite this version:

Nicolas Albar, Thomas Hérissou de Beauvoir, Aurélien Bouyat, Geoffroy Chevallier, Alicia Weibel, et al.. Master sintering curve analysis of ZnO densified by Cold Sintering Process. Open Ceramics, 2024, 18, pp.100593. 10.1016/J.OCERAM.2024.100593 . hal-04590368

**HAL Id: hal-04590368**

**<https://cnrs.hal.science/hal-04590368v1>**

Submitted on 13 Nov 2024

**HAL** is a multi-disciplinary open access archive for the deposit and dissemination of scientific research documents, whether they are published or not. The documents may come from teaching and research institutions in France or abroad, or from public or private research centers.

L'archive ouverte pluridisciplinaire **HAL**, est destinée au dépôt et à la diffusion de documents scientifiques de niveau recherche, publiés ou non, émanant des établissements d'enseignement et de recherche français ou étrangers, des laboratoires publics ou privés.



Distributed under a Creative Commons Attribution - NonCommercial - NoDerivatives 4.0 International License



# Master sintering curve analysis of ZnO densified by Cold Sintering Process

Nicolas Albar<sup>\*</sup>, Thomas Hérisson de Beauvoir, Aurélien Bouyat, Geoffroy Chevallier, Alicia Weibel, Claude Estournès

CIRIMAT, Université Toulouse 3 – Paul Sabatier, CNRS-INP-UPS, Université de Toulouse, France

## ARTICLE INFO

Handling editor: Dr P Colombo

### Keywords:

Sintering  
Master Sintering Curve  
Cold Sintering Process (CSP)

## ABSTRACT

The Master Sintering Curve (MSC) model is traditionally used to describe the densification kinetics of a specific material and allows to determine the activation energy of the dominant mechanism. In this study, this approach is applied to the Cold Sintering Process (CSP) of ZnO with the addition of acetic acid. The result was compared with SPS sintered samples from the same dry powder. The apparent activation energy of the ZnO powder sintered by CSP with acetic acid is 4 times lower than the same dry powder (338 kJ/mol versus 83 kJ/mol). This low value confirms the low energy surface interactions between liquid and solid phases involved in mechanisms of ZnO. MSC model applied to CSP presents different interests to detect similarities or differences in sintering mechanism with different liquid phases. It allows to determine the densification trajectory of the material, then to select the optimum processing parameters to control its microstructure.

## 1. Introduction

Sintering ceramics at low temperature has been an important objective pursued for decades. The development of techniques such as Hydrothermal Hot Pressing [1–3], Hydrothermal Sintering [4,5] but also Spark Plasma Sintering at low temperatures [6–8] have changed the way we considered sintering mechanisms and the possibilities offered in terms of material's processing. Among these techniques, the Cold Sintering Process (CSP) has proved incredible efficiency over a wide range of materials, including ceramics, polymers, and metals [9–12], but also new composite systems [13–15]. It has attracted a lot of attention due to the simplicity of the experimental setup and the interesting opportunities offered by the sintering mechanisms.

Despite this high efficiency, there are some limitations to the sintering capacities, mainly related to the dissolution-precipitation mechanisms that may lead to incongruent dissolution [16] and force the precipitation of undesired phase. Among these, the mechanisms are still under debate and appear more complex than initially postulated [17]. The development of fundamental understanding in the field of sintering mechanisms, including the solid/liquid interactions (complexation, cristallization, dissolution, transport, precipitation) can help controlling sintering. This could allow the densification in Cold Sintering of some refractory materials for instance, that often require a post annealing high temperature treatments [18,19]. Therefore, it can help the

development on single step Cold Sintering Process. However, after facing difficulties in finding solutions to avoid such treatments, it has recently been demonstrated the possibility to overcome the Cold Sintering issues by changing the sintering parameters and use ionic liquids instead of water based liquids for instance Refs. [20–22]. These examples demonstrated the necessity to master the sintering mechanisms to obtain targeted materials and microstructures to tailor the properties.

A major challenge in the case of CSP relates to the characterization and determination of sintering mechanisms. Different techniques were adapted to obtain *in situ* information about the materials facing sintering. *In situ* SAXS measurements [23,24] and impedance analyses [25,26] allowed to investigate the evolution of porosities and grain boundaries during and after Cold Sintering experiments. This type of characterization work is detrimental for further development of the CSP and helps to identify the underlying mechanisms.

Apart from that, a modeling approach can be greatly beneficial for both the understanding and the predictability of the sintering process. Examples of molecular dynamics simulations have shed light on interesting chemical reactions occurring at the solid-liquid interfaces [27–29]. Other modeling methods can provide information about the kinetics of both sintering and grain growth. As an example, anisothermal modeling application to CSP has brought information about the kinetic analysis of ZnO sintering [30]. This allows the determination of activation energy of sintering under various sintering conditions both in

<sup>\*</sup> Corresponding author.

E-mail address: [nicolas.albar@hotmail.com](mailto:nicolas.albar@hotmail.com) (N. Albar).

<https://doi.org/10.1016/j.oceram.2024.100593>

Received 13 March 2024; Received in revised form 5 April 2024; Accepted 10 April 2024

Available online 16 April 2024

2666-5395/© 2024 The Authors. Published by Elsevier Ltd on behalf of European Ceramic Society. This is an open access article under the CC BY-NC-ND license (<http://creativecommons.org/licenses/by-nc-nd/4.0/>).

terms of chemistry (liquid phase content, concentration, or nature, powder surface chemistry and crystallinity) or physical parameters (applied pressure, green body density or temperature).

Among the kinetic analysis models, the Master Sintering Curve (MSC), is an easy to use, rapid and versatile technique that can be applied to different sintering techniques, on the basis of dilatometric data. The method, first introduced by Su & Johnson [31], allows to obtain activation energy of sintering, and was yet never applied to Cold Sintering. It could bring interesting information about the sintering kinetics, allow to quantify the influence of materials and processing parameters on the sintering activation energies. In the present work, the model is applied to the sintering in SPS apparatus of ZnO in the presence of acetic acid and dry ZnO for the sake of comparison.

## 2. Experimental

The starting powder used in this work is a ZnO powder commercially available from Alfa Aesar, NanoArc (>99 %) with a particle size in the range 40–100 nm. A 1 M acetic acid solution in distilled water was prepared from Sigma Aldrich glacial acetic acid (>99 %). For the sintering experiments, 1 g of ZnO powder was mixed with 0.3 mL of 1 M acetic acid solution and manually mixed in a mortar. After 5 min of manual mixing, the powder was placed in a 8 mm diameter WC-Co die. To prevent direct contact between the die and the powder, a 0.2 mm graphite foil (PERMAFOIL®Toyo Tanso) was placed between the powder and each punch, but also vertically between the inner wall of the mold and the powder.

Sintering experiments were performed in a Spark Plasma Sintering (SPS) apparatus (FUJI 632Lx from Fuji Electronic Industrial CO., Japan) using pulsed DC sources, located at the *Plateforme Nationale CNRS de Frittage Flash* at the University of Toulouse. Temperature was monitored using a K type thermocouple placed in a hole halfway up the external surface of the die. Typical CSP setup does not allow the application of high temperature ramps (>20–30 °C/min) and therefore the use of SPS was chosen to overcome this technical limitation. Therefore, the use of the term CSP-SPS will be used to clarify this point throughout the manuscript. Pressure application is controlled by the SPS equipment, along with dilatometric measurements that is performed during the whole sintering experiment. The sample was first put under a mechanical pressure of 100 MPa in vacuum atmosphere (≈10 Pa) or in air at room temperature and left to stabilize the pressure related displacement for 1 min at room temperature and reach the green density ( $\rho_0$ ). Then, temperature ramp (20 °C/min, 50 °C/min and 100 °C/min) was applied to reach the maximum temperature at 300 °C.

Classical SPS experiments were processed in the same conditions than for the CSP-SPS on dry ZnO powder and the maximum dwell temperature reached 600 °C. A blank measurement was made on the whole setup after sintering to remove contribution from the thermal expansion of the column (sample + punches + spacers). This blank analysis allowed the correction of the dilatometric data to only consider the shrinkage of the powder compact. Density measurements were further made on sintered specimens by geometrical shape measurements and weighting. The obtained data were compared to the theoretical ZnO density of 5.606 g/cm<sup>3</sup> to determine the relative density.

## 3. Results

CSP usually relies on the application of a low temperature (<400 °C) on a sample placed in a die submitted to a significant uniaxial mechanical pressure (0.1–1 GPa). The die heating is achieved by placing a heater jacket around the die (Fig. 1). This setup usually limits the heating rates to values < 30 °C/min. However, Dargatz et al. [32] demonstrated the heating rate in the range 10–200 °C/min may have a strong influence on ZnO densification in the presence of water. To perform CSP experiments under such high heating rates (up to 100 °C/min), they used a SPS device allowing Joule heating from

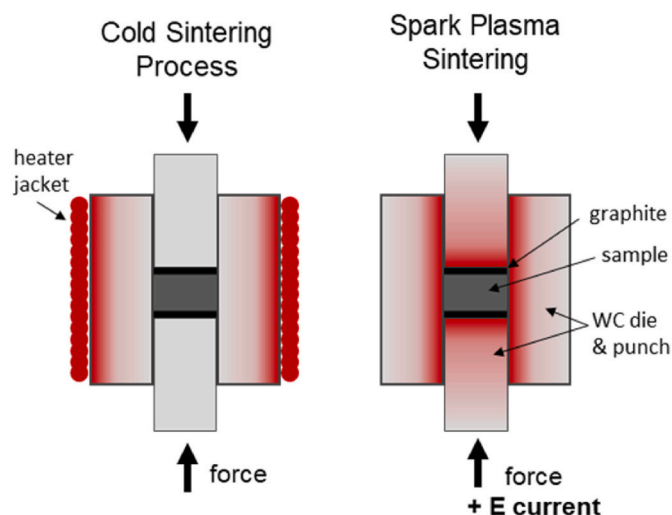


Fig. 1. Schematic view of the Cold Sintering Process and Spark Plasma Sintering setups. Red coloration represents the temperature gradients in the die and punches.

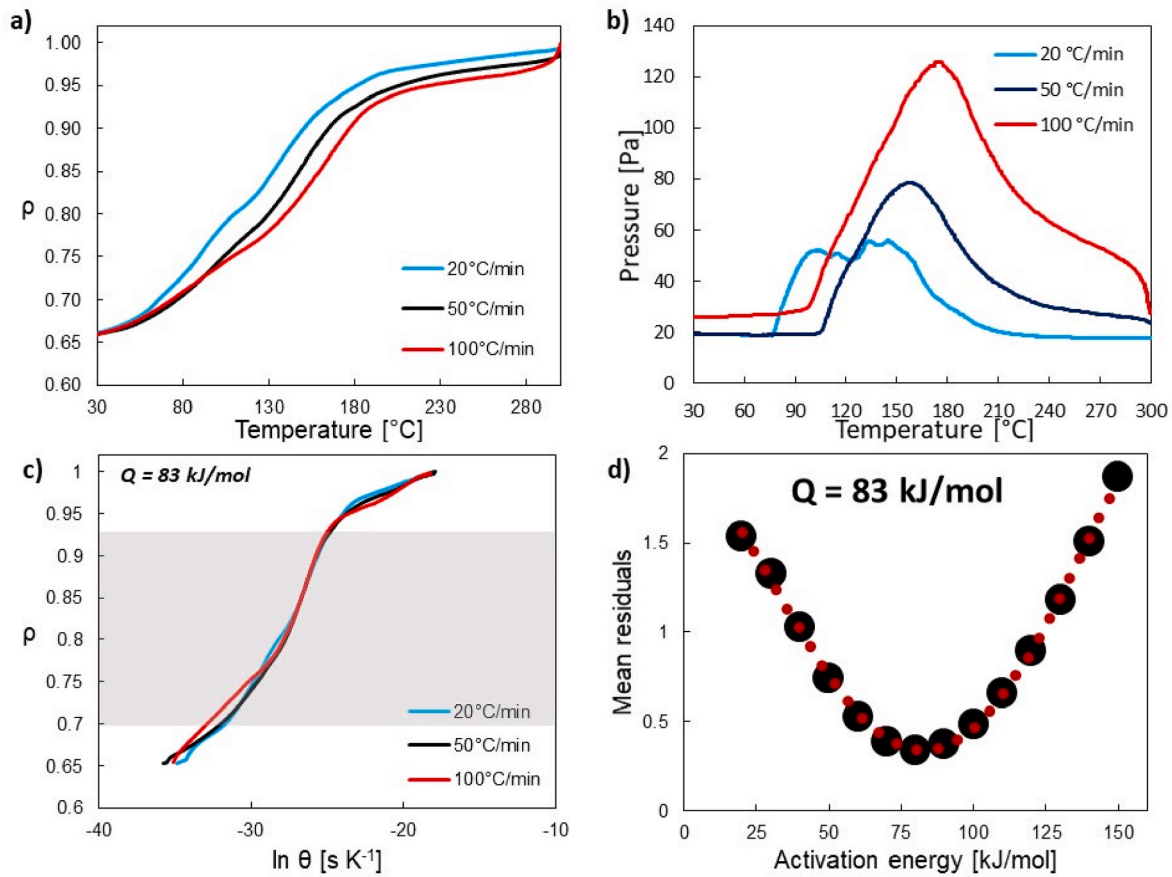
electrical current to heat the sample. This setup may present differences in temperature gradients compared to conventional CSP. This way, the temperature gradient is reversed and the maximum temperature must be found near the sample. Although this may not represent a problem in terms of sintering mechanisms, this must be taken in consideration when assessing the results differences between the two setups, leading to a slight temperature shift. Considering the current flow, our previous studies about the *in operando* impedance characterizations of the same powder/liquid preparation lead to the observation of resistivity in the range of  $10^2 \Omega \text{ cm}$  [25,26], which must force the current flow through the conductive WC-Co die instead of going through the sample. Therefore, the effect of current flow through the sample may be neglected in the case of CSP-SPS of ZnO with acetic acid.

Fig. 2a shows the evolution of the relative density as a function of temperature for the different heating ramps. The higher the heating rate, the more the densification of the material is shifted towards higher temperatures. This phenomenon can be explained by the different thermal history of the material as a function of the temperature ramp which is translated by the sintering work  $\theta$  described by equation (1) [33] reported below.

$$\theta = \int_0^t \frac{1}{T} \exp\left(\frac{-Q}{RT}\right) dt \quad (1)$$

where  $\theta$ , the work of sintering, is expressed as a function of temperature  $T$ , time  $t$  and the activation energy  $Q$ .  $R$  is the gas constant. Fig. 2 b corresponds to the pressure into the SPS chamber during the sintering and can be correlated with degassing of the liquid phase. When the degassing is very significant we have a displacement, which is not associated with densification but with the elimination of the liquid phase, we therefore see for each curve in Fig. 2 a that there is a break in slope around 130 °C which is associated with the elimination of part of the liquid phase. Fig. 2 c represents the evolution of the relative density as a function of  $\ln(\theta)$ . One can observe that the three curves nearly superimposed in the whole  $\ln(\theta)$  range explored, which indicates that a single sintering mechanism operates in such conditions, whose apparent activation energy was determined to be 83 kJ/mol with the Mean Residuals curve [34] as shown in Fig. 2 d. These residuals were obtained from values between 70 % and 93 % relative density.

In order to make a comparison with CSP-SPS experiments, a MSC analysis was performed on dry ZnO powder sintered by SPS at 600 °C using the same thermal ramps (20,50 and 100 °C/min). Fig. 3 shows the densification curves with temperature and the calculated MSC values



**Fig. 2.** a) Densification curves plotted at different heating rates, b) Pressure in the SPS chamber at different heating rate c) Relative density vs.  $\ln \theta$  for  $Q_{MSC} = 83$  kJ/mol determined between 70 % and 93 % of relative density and d) Mean residuals calculated for various apparent activation energies.

using  $\theta$  values from 80 % to 92 % of relative density. In presence of acetic acid solution, we almost reach a densification plateau around 200 °C by CSP-SPS while by conventional SPS on the same powder without liquid phase, the plateau is reached at 480 °C. In the latter case, the Mean Residuals method gives an apparent activation energy of 338 kJ/mol, which is more than 4 times the apparent activation energy determined in the case of the wetted powder with the acetic acid solution densified by CSP-SPS. The densification mechanisms are different; from chemically-driven low temperature CSP-SPS to thermally activated solid state diffusion in SPS.

One of the advantages of the MSC analysis relies on its ability to predict the shrinkage behavior of a material at any given temperature ramp. To model this shrinkage, sintering work ( $\theta$ ) must be related to the relative density over time ( $\rho(t)$ ) using  $\Psi$  and  $\phi$  parameters defined by equations 2 and 3 [33,35], respectively.

$$\Psi = \frac{\rho - \rho_0}{1 - \rho_0} = \frac{1}{1 + \exp\left[-\frac{\ln(\theta) - \ln(\theta_{ref})}{n}\right]} \quad (2)$$

$$\phi = \frac{\rho - \rho_0}{1 - \rho} = \left(\frac{\theta}{\theta_{ref}}\right)^{1/n} \quad (3)$$

Where  $\rho_0$  is the initial relative density of the powder compact or green body,  $\rho$  its relative density during sintering,  $\ln(\theta_{ref})$  corresponds to the sintering process halfway through densification and  $n$  is a power law exponent correlated with the sintering mechanism. To determine  $n$  value, Blaine et al. [33,35] proposed a linearization method for the MSC according to equation (4).

$$\ln(\phi) = \frac{1}{n} (\ln(\theta) - \ln(\theta_{ref})) \quad (4)$$

The plot of  $\ln(\phi) = f(\ln(\theta))$  using equation (4) is presented in Fig. 4 a. The slope gives  $n$  value equal to 2.2 for CSP of ZnO powder with acetic acid solution. Using this value of  $n$  and  $Q = 83$  kJ/mol, it is possible to plot the densification parameter  $\Psi$  as a function of  $\ln(\theta)$ , independently of the temperature ramp. Fig. 4 b shows that the model is valid for all the sintering curves obtained for heating rates ranging from 20 to 100 °C/min. With this model, it is thus possible to predict the relative density of the material during the whole sintering cycle.

#### 4. Discussion

We demonstrated that MSC analysis is valid for the determination of CSP-SPS kinetics of ZnO with acetic acid. ZnO is used as a model material, since it has a great ability to sinter at low temperature in various solvents such as pure water, acetic acid, formic acid or citric acid [9,32, 36]. The fact that all the data can be fitted with a single master sintering curve for the whole temperature ramps explored is a confirmation that the sintering mechanism involved in the sintering of ZnO wetted with a 1 M acetic acid solution is not affected by the temperature ramp. This has to be put in comparison with the work from Dargatz et al. [32] showing the influence of heating rate by activation of low temperature sintering mechanism on hydrated ZnO sintered by SPS at heating rates >50 K/min. They have highlighted an activation energy of 130 kJ/mol, attributed to a better thermal diffusion and temperature homogeneity compared with a dry powder. This value is slightly higher than 83 kJ/mol found in our experiments using acetic acid solution. This confirms the role played by acetic acid solution, serving as a sintering

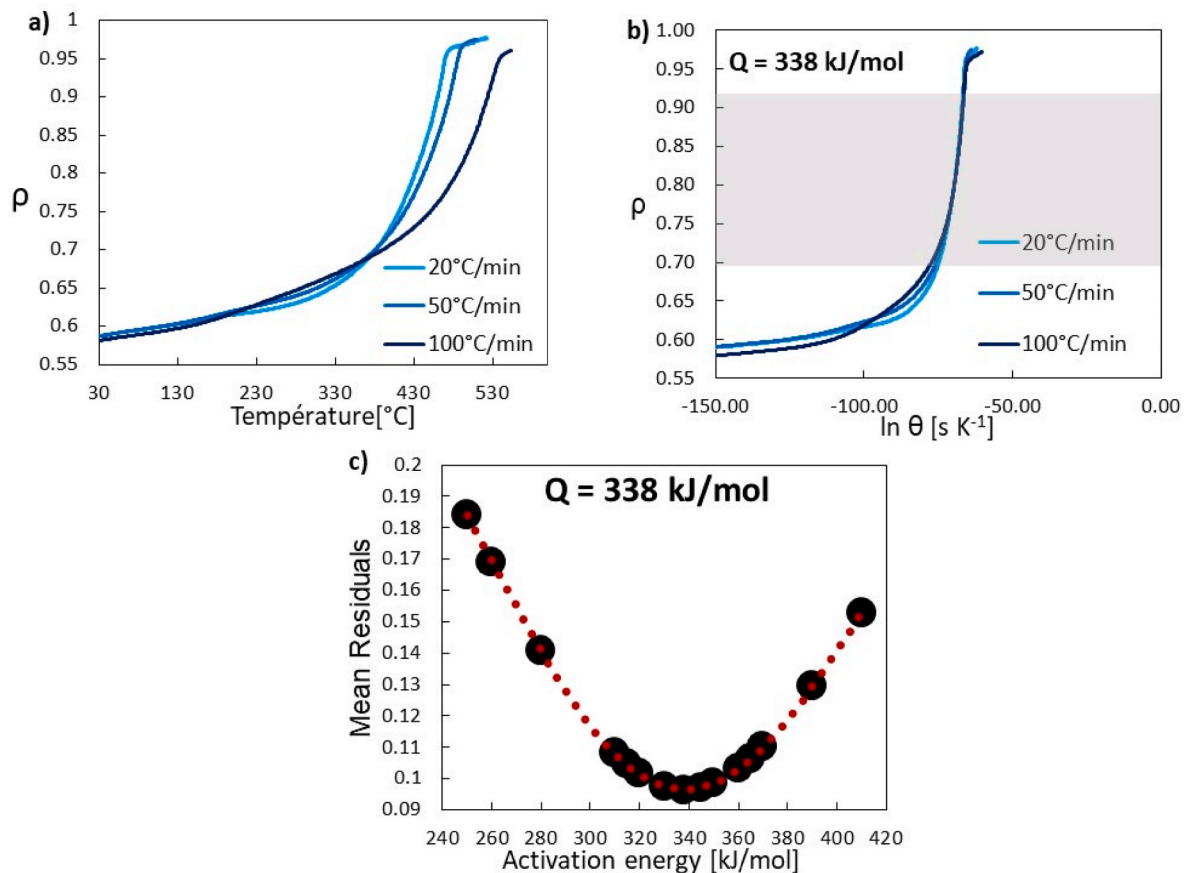


**Fig. 3.** a) Densification curves plotted at different heating rates, b) Relative density vs.  $\ln \theta$  for  $Q_{\text{MSC}} = 338 \text{ kJ/mol}$  determined between 70 % and 92 % of relative density and c) Means residuals calculated for various apparent activation energies.

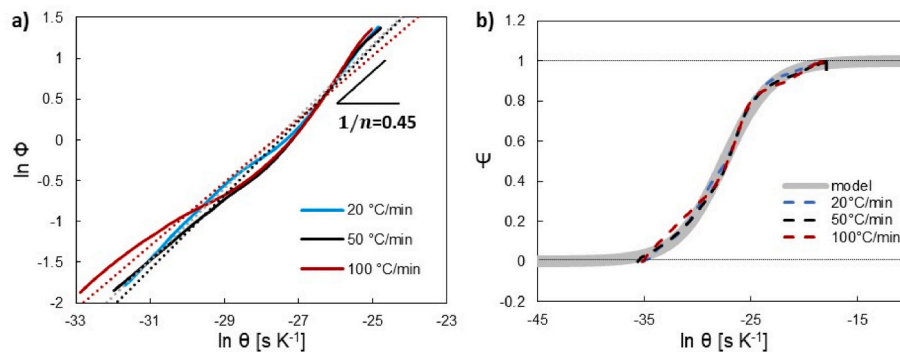


**Fig. 4.** a) Linearization of the parameter  $\phi$  to determine  $a$  and  $n$  and b)  $\Psi = f(\ln(\theta))$  of fitted model and experimental curves.

accelerator for ZnO as compared to pure water. However, these values must be considered with caution since the MSC activation energy depends on the whole processing parameters, including powder granulometry/morphology. The activation energy would probably be slightly affected by using a different powder.

To tackle this issue, experiments were also performed using the same ZnO powder, without any liquid phase during sintering. These conventional SPS experiments allowed a direct comparison of the MSC apparent activation energy results, showing a shift from 83 to 338 kJ/mol. This indicates that SPS processed samples, in dry conditions, are much more affected by the heating rates than the CSP-SPS samples. This also confirms a huge difference in the mechanisms involved during sintering in such different conditions. As it could be expected, the apparent activation energies from the lowest to largest value correspond to  $Q$  (CSP-SPS

acetic acid)  $< Q$  (SPS hydrated)  $< Q$  (SPS dry), showing the effect of liquid phase effects during sintering. These data are also consistent with the observations made by Bang et al. [30] when using anisothermal kinetic analysis models to determine sintering activation energies of ZnO sintered by CSP in the presence of pure water and various acetic acid concentrations. They found an activation energy of  $68 \pm 9 \text{ kJ/mol}$  at a heating ramp of 15  $^{\circ}\text{C}/\text{min}$ , for an acetic acid solution of 2 mol/L, using the Woolfrey-Bannister method. Such low energies can be related to the chemically-driven solution-precipitation sintering mechanisms involved in the CSP.

These kinetic studies, especially applied to CSP, present 3 main interests.



- The possibility to detect similarities or differences in sintering mechanisms (activation or inhibition) by the use of kinetic analysis; the work of Dargatz et al. [32] is a great example of high thermal ramp effect on the activation of sintering mechanism of ZnO in the presence of water.
- The possibility to determine densification curves for any conditions of time and temperature, leading to the possibility to obtain desired microstructures.
- The capacity to quantify, using  $n$  and  $Q$  values, the effect of processing parameters on the kinetics of sintering.

This way, this work highlights the possibility to evaluate the role of the numerous processing parameters on the sintering kinetics. This is particularly important in the case of CSP-SPS and more generally for CSP, involving more parameters than the other sintering processes, due to the presence of a liquid phase (nature of liquid, quantity, concentration, elimination temperatures, ...).

## 5. Conclusions

This work focuses on the MSC model applied to the sintering of ZnO by CSP with acetic acid. This highlights the fact that MSC can be applied in the case of CSP, and allows the determination of apparent activation energy and  $n$  exponent, related to the governing sintering mechanism. The apparent activation energy determined for a dry powder in SPS sintering is around 340 kJ/mol. Dargatz et al. [32] have evidenced a change of sintering mechanism associated with a lower activation energy of 130 kJ/mol for the CSP-SPS of ZnO with the addition of water. If 1 M acetic acid solution is used, the apparent activation energy decreases to 83 kJ/mol. It is shown that the use of a different liquid phase makes it possible to modify the apparent activation energy of the densification mechanism involved during sintering. Using acetic acid in which ZnO is the most soluble seems to have a strong influence on the apparent activation energy of the sintering mechanism involved. This work paves the way to more predictive studies of CSP of various materials, and the analysis of the relative influence of various sintering parameters.

## CRediT authorship contribution statement

**Nicolas Albar:** Data curation, Investigation, Writing – original draft. **Thomas Hérisson de Beauvoir:** Conceptualization, Data curation, Writing – original draft. **Aurélien Bouyat:** Investigation. **Geoffroy Chevallier:** Investigation, Writing – review & editing. **Alicia Weibel:** Writing – review & editing. **Claude Estournès:** Supervision, Writing – review & editing.

## Declaration of competing interest

The authors declare that they have no known competing financial interests or personal relationships that could have appeared to influence the work reported in this paper.

The author is an Editorial Board Member/Editor-in-Chief/Associate Editor/Guest Editor for *Open Ceramics* and was not involved in the editorial review or the decision to publish this article.

## References

- [1] N. Yamasaki, K. Yanagisawa, M. Nishioka, S. Kanahara, A hydrothermal hot-pressing method: apparatus and application, *J. Mater. Sci. Lett.* 5 (1986) 355–356.
- [2] K. Yanagisawa, M. Nishioka, K. Ioku, N. Yamasaki, Densification of silica gels by hydrothermal hot-pressing, *J. Mater. Sci. Lett.* 12 (1993) 1073–1075.
- [3] K. Yanagisawa, K. Ioku, N. Yamasaki, Post-sintering of anatase compact prepared by hydrothermal hot-pressing, *J. Mater. Sci. Lett.* 14 (1995) 161–163.
- [4] G. Goglio, A. Ndayishimiye, A. Largeau, C. Elissalde, View point on hydrothermal sintering: main features, today's recent advances and tomorrow's promises, *Scripta Mater.* 158 (2019) 146–152, <https://doi.org/10.1016/j.scriptamat.2018.08.038>.
- [5] A. Ndayishimiye, A. Largeau, S. Mornet, M. Duttine, M.-A. Dourges, D. Denux, M. Verdier, M. Goune, T. Herisson de Beauvoir, C. Elissalde, G. Goglio, Hydrothermal sintering for densification of silica. Evidence for the role of water, *J. Eur. Ceram. Soc.* 38 (2018) 1860–1870, <https://doi.org/10.1016/j.jeurceramsoc.2017.10.011>.
- [6] C. Drouet, C. Largeot, G. Raimbeaux, C. Estournès, G. Dechambre, C. Combes, C. Rey, Bioceramics: spark plasma sintering (SPS) of Calcium Phosphates, *Adv. Sci. Technol.* 49 (2006) 45–50, <https://doi.org/10.4028/www.scientific.net/ast.49.45>.
- [7] F. Brouillet, D. Laurencin, D. Grossin, C. Drouet, C. Estournès, G. Chevallier, C. Rey, Biomimetic apatite-based composite materials obtained by spark plasma sintering (SPS): physicochemical and mechanical characterizations, *J. Mater. Sci. Mater. Med.* 26 (2015) 1–11.
- [8] Catherine Elissalde, U-Chan Chung, Michaël Josse, Graziella Goglio, Matthew R. Suchomel, Jérôme Majimel, Alicia Weibel, F. Soubie, Andréas Flaureau, Arnaud Fregeac, Estournès, Claude Single-step sintering of zirconia ceramics using hydroxide precursors and spark plasma sintering below 400°C, *Scripta Mater.* 168 (2019) 134–138, ISSN 1359-6462.
- [9] S. Funahashi, J. Guo, H. Guo, K. Wang, A.L. Baker, K. Shiratsuyu, C.A. Randall, Demonstration of the cold sintering process study for the densification and grain growth of ZnO ceramics, *J. Am. Ceram. Soc.* 100 (2017) 546–553, <https://doi.org/10.1111/jace.14617>.
- [10] T. Herisson de Beauvoir, S. Dursun, L. Gao, C. Randall, New opportunities in Metallization Integration in Cofired Electroceramic Multilayers by the cold sintering process, *ACS Appl. Electron. Mater.* 1 (2019) 1198–1207, <https://doi.org/10.1021/acsaem.9b00184>.
- [11] T. Hérisson de Beauvoir, K. Tsuji, X. Zhao, J. Guo, C. Randall, Cold sintering of ZnO-PTFE: Utilizing polymer phase to promote ceramic anisotropic grain growth, *Acta Mater.* 186 (2020), <https://doi.org/10.1016/j.actamat.2020.01.002>.
- [12] S. Funahashi, H. Guo, J. Guo, A.L. Baker, K. Wang, K. Shiratsuyu, C.A. Randall, Cold sintering and co-firing of a multilayer device with thermoelectric materials, *J. Am. Ceram. Soc.* 100 (2017) 3488–3496, <https://doi.org/10.1111/jace.14852>.
- [13] S. Dursun, K. Tsuji, S.H. Bang, A. Ndayishimiye, C.A. Randall, A Route towards Fabrication of functional ceramic/polymer Nanocomposite devices using the cold sintering process, *ACS Appl. Electron. Mater.* (2020), <https://doi.org/10.1021/acsaem.0c00225>.
- [14] J. Guo, S.S. Berbano, H. Guo, A.L. Baker, M.T. Lanagan, C.A. Randall, Cold sintering process of composites: Bridging the processing temperature gap of ceramic and polymer materials, *Adv. Funct. Mater.* 26 (2016) 7115–7121.
- [15] J. Guo, B. Legum, B. Anasori, K. Wang, P. Lelyukh, Y. Gogotsi, C.A. Randall, Cold sintered ceramic Nanocomposites of 2D MXene and zinc oxide, *Adv. Mater.* 30 (2018) 1801846, <https://doi.org/10.1002/adma.201801846>.
- [16] Y. Huang, K. Huang, S. Zhou, C. Lin, X. Wu, M. Gao, C. Zhao, C. Fang, Influence of incongruent dissolution-precipitation on 8YSZ ceramics during cold sintering process, *J. Eur. Ceram. Soc.* 42 (2022) 2362–2369, <https://doi.org/10.1016/j.jeurceramsoc.2021.12.072>.
- [17] S. Grasso, M. Biesuz, L. Zoli, G. Taveri, A.I. Duff, D. Ke, A. Jiang, M.J. Reece, A review of cold sintering processes, *Adv. Appl. Ceram.* 119 (2020) 115–143, <https://doi.org/10.1080/17436753.2019.1706825>.
- [18] H. Guo, J. Guo, A. Baker, C.A. Randall, Cold sintering process for ZrO<sub>2</sub>-based ceramics: Significantly Enhanced densification evolution in Ytria-Doped ZrO<sub>2</sub>, *J. Am. Ceram. Soc.* 100 (2017) 491–495, <https://doi.org/10.1111/jace.14593>.
- [19] K. Thabet, E. Quarez, O. Joubert, A. Le Gal La Salle, Application of the cold sintering process to the electrolyte material BaCe<sub>0.8</sub>Zr<sub>0.1</sub>Y<sub>0.1</sub>O<sub>3-δ</sub>, *J. Eur. Ceram. Soc.* 40 (2020) 3445–3452, <https://doi.org/10.1016/j.jeurceramsoc.2020.03.043>.
- [20] K. Tsuji, A. Ndayishimiye, S. Lowum, R. Floyd, K. Wang, M. Wetherington, J. Maria, C.A. Randall, Single step densification of high Permittivity BaTiO<sub>3</sub> ceramics at 300 °C, *J. Eur. Ceram. Soc.* 40 (2020) 1280–1284, <https://doi.org/10.1016/j.jeurceramsoc.2019.12.022>.
- [21] T.H. Zaengle, A. Ndayishimiye, K. Tsuji, Z. Fan, S.H. Bang, J. Perini, S.T. Misture, C.A. Randall, Single-step densification of nanocrystalline CeO<sub>2</sub> by the cold sintering process, *J. Am. Ceram. Soc.* 103 (2020) 2979–2985, <https://doi.org/10.1111/jace.17003>.
- [22] T. Sada, Z. Fan, A. Ndayishimiye, K. Tsuji, S.H. Bang, Y. Fujioka, C.A. Randall, In situ doping of BaTiO<sub>3</sub> and visualization of pressure solution in flux-assisted cold sintering, *J. Am. Ceram. Soc.* 104 (2021) 96–104, <https://doi.org/10.1111/jace.17461>.
- [23] A.J. Allen, I. Levin, R.A. Maier, S.E. Witt, F. Zhang, I. Kuzmenko, In situ characterization of ceramic cold sintering by small-angle scattering, *J. Am. Ceram. Soc.* 104 (2021) 2442–2448, <https://doi.org/10.1111/jace.17664>.
- [24] F. Zhang, R.A. Maier, I. Levin, A.J. Allen, J.S. Park, P. Kenesei, I. Kuzmenko, P. Jemian, J. Ilavsky, In situ probing of interfacial roughness and transient phases during ceramic cold sintering process, *Acta Mater.* 259 (2023), <https://doi.org/10.1016/j.actamat.2023.119283>.
- [25] T. Hérisson de Beauvoir, P.L. Taberna, P. Simon, C. Estournès, Cold Sintering Process characterization by in operando electrochemical impedance spectroscopy, *J. Eur. Ceram. Soc.* 42 (2022) 5747–5755, <https://doi.org/10.1016/j.jeurceramsoc.2022.05.077>.
- [26] T. Hérisson de Beauvoir, C. Estournès, Room temperature ZnO ageing after Cold Sintering Process: grain boundaries evolution characterization by *in situ* electrochemical impedance spectroscopy, *J. Eur. Ceram. Soc.* (2024), <https://doi.org/10.1016/j.jeurceramsoc.2024.02.014>.
- [27] M.Y. Sengul, C.A. Randall, A.C.T. Van Duin, ReaxFF molecular dynamics study on the influence of temperature on Adsorption, Desorption, and Decomposition at the acetic acid/water/ZnO(1010) interface Enabling cold sintering, *ACS Appl. Mater. Interfaces* 10 (2018) 37717–37724, <https://doi.org/10.1021/acsaami.8b13630>.
- [28] M.Y. Sengul, J. Guo, C.A. Randall, A.C.T. van Duin, Water-mediated surface diffusion mechanism Enables the cold sintering process: a Combined

- Computational and experimental study, *Angew. Chem. Int. Ed.* 58 (2019) 12420–12424, <https://doi.org/10.1002/anie.201904738>.
- [29] A. Ndayishimiye, M.Y. Sengul, S.H. Bang, K. Tsuji, K. Takashima, T. Hérisson de Beauvoir, D. Denux, J.M. Thibaud, A.C.T. van Duin, C. Elissalde, G. Goglio, C. A. Randall, Comparing hydrothermal sintering and cold sintering process: mechanisms, microstructure, kinetics and chemistry, *J. Eur. Ceram. Soc.* 40 (2020) 1312–1324, <https://doi.org/10.1016/j.jeurceramsoc.2019.11.049>.
- [30] S.H. Bang, A. Ndayishimiye, C.A. Randall, Anisothermal densification kinetics of the cold sintering process below 150 °C, *J. Mater. Chem. C* 8 (2020) 5668–5672, <https://doi.org/10.1039/D0TC00395F>.
- [31] H. Su, D.L. Johnson, Master sintering curve: a Practicle approach to sintering, *J. Am. Ceram. Soc.* 79 (1996) 3211–3217.
- [32] B. Dargatz, J. Gonzalez-Julian, M. Bram, P. Jakes, A. Besmehn, L. Schade, R. Röder, C. Ronning, O. Guillon, FAST/SPS sintering of nanocrystalline zinc oxide—Part I: Enhanced densification and formation of hydrogen-related defects in presence of adsorbed water, *J. Eur. Ceram. Soc.* 36 (2016) 1207–1220, <https://doi.org/10.1016/j.jeurceramsoc.2015.12.009>.
- [33] D.C. Blaine, S.-J. Park, R.M. German, Linearization of master sintering curve, *J. Am. Ceram. Soc.* 92 (2009) 1403–1409, <https://doi.org/10.1111/j.1551-2916.2009.03011.x>.
- [34] V. Pouchly, K. Maca, Master sintering curve – a Practical approach to its Construction, *Sci. Sinter.* (2010).
- [35] D.C. Blaine, S. Park, R.M. German, Master Sintering Curve for a Two-phase Material, Center for Innovative Sintered Products, The Pennsylvania State University, University Park, PA, USA...
- [36] A. Jabr, J. Fanghanel, Z. Fan, R. Bermejo, C. Randall, The effect of liquid phase chemistry on the densification and strength of cold sintered ZnO, *J. Eur. Ceram. Soc.* 43 (2023) 1531–1541, <https://doi.org/10.1016/j.jeurceramsoc.2022.11.071>.